



Effect of archaeal lipids from *A. pernix* K1 on the *in vitro* stability and active loading efficiency of liposomes composed of sphingomyelin and cholesterol

Jan Kejžar, Mihaela Skrt, Tamara Polajžer & Nataša Poklar Ulrih

To cite this article: Jan Kejžar, Mihaela Skrt, Tamara Polajžer & Nataša Poklar Ulrih (01 Feb 2026): Effect of archaeal lipids from *A. pernix* K1 on the *in vitro* stability and active loading efficiency of liposomes composed of sphingomyelin and cholesterol, Journal of Liposome Research, DOI: [10.1080/08982104.2026.2619597](https://doi.org/10.1080/08982104.2026.2619597)

To link to this article: <https://doi.org/10.1080/08982104.2026.2619597>



© 2026 The Author(s). Published by Informa UK Limited, trading as Taylor & Francis Group



Published online: 01 Feb 2026.



Submit your article to this journal [↗](#)



Article views: 367



View related articles [↗](#)



View Crossmark data [↗](#)

Effect of archaeal lipids from *A. pernix* K1 on the *in vitro* stability and active loading efficiency of liposomes composed of sphingomyelin and cholesterol

Jan Kejžar^a, Mihaela Skrt^a, Tamara Polajžer^b and Nataša Poklar Ulrih^{a,c}

^aDepartment of Food Science and Technology, Biotechnical Faculty, University of Ljubljana, Ljubljana, Slovenia; ^bLaboratory of Biocybernetics, Faculty of Electrical Engineering, University of Ljubljana, Ljubljana, Slovenia; ^cThe Centre of Excellence for Integrated Approaches in Chemistry and Biology of Proteins (CipKeBiP), Ljubljana, Slovenia

ABSTRACT

Archaeal lipids offer a useful strategy for improving liposomal systems because of their inherent stability under extreme conditions. Incorporating lipids from *Aeropyrum pernix* K1 allowed us to optimize sphingomyelin-cholesterol formulation. These archaeal lipids enabled complete recovery of liposome morphology after destabilization with 4 mM Ca²⁺ followed by EDTA, indicating that membrane integrity is maintained in the presence of calcium. This is noteworthy given the anionic nature of the archaeal lipids, which in this case provide colloidal stability without increasing sensitivity to Ca²⁺. The addition of 2 mol% archaeal lipids also supported high encapsulation efficiency of 95% for active vincristine loading and performed better than the binary mixture when vesicles were prepared by extrusion without cosolvents. Furthermore, reducing the archaeal lipid fraction preserved biological stability provided by sphingomyelin-cholesterol, as confirmed by flow cytometry and fluorescence microscopy, whereas pure archaeosomes composed entirely of archaeal lipids have been reported to show poor stability in biological systems.

ARTICLE HISTORY

Received 11 December 2025
Revised 5 January 2026
Accepted 8 January 2026

KEYWORDS

Archaea; lipids; liposomes; drug delivery systems; stability; vincristine

Introduction

Liposomes are defined as microscopic spherical structures composed of phospholipid bilayers, enabling efficient delivery of both hydrophilic and hydrophobic compounds [1]. Despite numerous advancements, such as the addition of cholesterol or polyethylene glycol (PEG) conjugates, their stability in biological systems remains one of the major limitations, which cannot be fully resolved with current methods.

A promising strategy to enhance liposomal stability is the replacement of conventional lipids with archaeal lipids. These lipids originate from *Archaea*, a distinct domain of prokaryotic microorganisms adapted to extreme environmental conditions, including high temperatures, elevated pressure, and extreme salinity or pH [2].

Their unique membrane lipids exhibit enhanced stability due to a combination of distinctive structural features [3,4], making them attractive for biotechnological and pharmaceutical applications [5]. This stability derives from ether linkages that are more chemically robust than ester bonds over a broad pH range, saturated alkyl chains resistant to oxidative degradation, and methyl side groups that reduce membrane permeability and lower the phase transition temperature. In addition, archaeal lipids possess the unusual *sn*-glycerol-1-phosphate backbone, the enantiomer of *sn*-glycerol-3-phosphate, which confers resistance to hydrolysis by certain phospholipases.

Particularly promising is their use in the development of stable liposomal drug delivery systems, where they can fully

or partially replace conventional phospholipids. Incorporating these lipids could significantly enhance the stability and efficacy of liposomes, broadening their applicability in various therapeutic and technological fields.

Among the most promising archaeal lipids are those derived from the archaeon *A. pernix*, which, due to their exceptional physicochemical stability and resistance to extreme conditions, present a potential solution for enhancing the stability of liposomal formulations. The hyperthermophilic archaeon *A. pernix* thrives at temperatures up to 100°C and was first isolated from a hydrothermal vent in Japan. Its polar lipids, particularly C_{25,25}-archetidyl(glucosyl)inositol (AGI) and C_{25,25}-archetidylinositol (AI), have emerged as promising components for developing stable drug delivery systems (Figure 1).

Preliminary studies have demonstrated that archaeosomes composed of 100 mol% C_{25,25} lipids exhibit exceptional physicochemical properties, including remarkable stability and non-toxicity in *in vitro* environments [6,7]. Despite these promising results, archaeosomes derived from *A. pernix* lipids have shown certain limitations. Key challenges include their stability in biological systems [8], incomplete characterization of these systems, and unverified capability for active loading of therapeutic agents.

In our previous study, we incorporated *A. pernix* lipids (C_{25,25}) into a well-established liposomal system composed of egg sphingomyelin (SM) and cholesterol (CH), a formulation widely used in both research and commercial settings due to

its proven efficacy and structural stability. We demonstrated that the resulting ternary SM:CH:C_{25,25} system supports the formation of monodisperse liposomes without the use of cosolvents [9]. These vesicles maintained morphological integrity across all tested lipid ratios, remained stable at elevated temperatures (up to 90 °C), and retained their structure during prolonged storage at 4 °C. Notably, the exceptional physicochemical stability of C_{25,25} lipids was preserved even at low concentrations. Incorporation of C_{25,25} lipids enabled the formation of small unilamellar vesicles (SUVs) by sonication, which was not possible with the SM:CH system alone. The addition of only 2–5 mol% C_{25,25} lipids decreased the zeta potential below –30 mV, thereby enhancing colloidal stability.

In this study, we focus on evaluating the *in vitro* stability of hybrid liposomes while seeking to overcome a key drawback of pure C_{25,25} archaeosomes, which is limited stability under physiologically relevant conditions [8].

Materials and methods

Chemicals

All chemicals used in the present study were from Sigma-Aldrich (St. Louis, MO, USA) unless specified otherwise. Egg sphingomyelin (>99% purity; 710.965 g/mol average

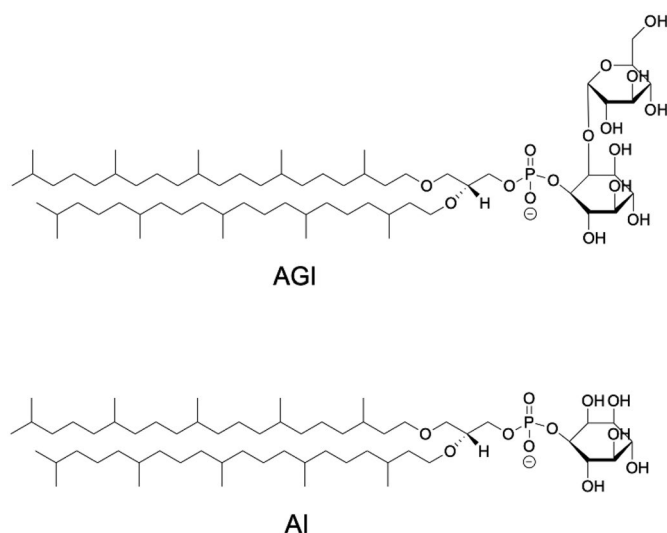


Figure 1. Structural formulas of 2,3-di-*O*-esterpanyl-*sn*-glycerol-1-phospho-1'-(2'-*O*- α -D-glucosyl)-myo-inositol (C_{25,25}-archetidyl(glucosyl)inositol) (AGI) and 2,3-di-*O*-esterpanyl-*sn*-glycerol-1-phospho-myo-inositol (C_{25,25}-archetidylinositol) (AI).

molecular weight; Lot:5869PQD118) was purchased from Avanti (Alabaster, AL, USA).

Preparation of large unilamellar vesicles (LUVs) via extrusion

To conduct this study, we followed the procedures developed in previous studies of *A. pernix* growth, harvesting and membrane lipid extraction [6,10]. Composition of *A. pernix* polar lipid fraction was determined by nuclear magnetic resonance and mass spectroscopy studies to have a constant ratio of 91 mol% AGI and 9 mol% AI [11]. Additionally, we confirmed the presence of AGI and AI of each new batch of isolated polar lipids by using adsorption chromatography and analyzed by TLC using chloroform/methanol/acetic acid/water (85/30/15/5 volumetric ratio) solvent (Appendix 1) as described by Ota et al. (2012) [12]. Furthermore, isolated polar lipids from *A. pernix* were also determined by LC-MS, revealing two major peaks corresponding to AGI and AI, respectively (Appendix 2).

Two types of vesicles were prepared in our study, small unilamellar vesicles (SUVs) and large unilamellar vesicles (LUVs). The variations in tested lipid compositions included different mol% of archaeal C_{25,25} lipids: 0%, 2%, 5%, 15%, 25%, 35%, and 45%, while keeping the molar ratio of egg sphingomyelin (SM) and cholesterol (CH) constant at 1.5 to 1 and using 100% sphingomyelin as control. Exact lipid compositions of liposome samples are provided in Table 1.

Liposome preparation and encapsulation

Multilamellar vesicles (MLVs) were prepared using the thin-film hydration method with selected lipid compositions. Dried lipid films were hydrated with one of the following aqueous solutions, depending on the intended application: 80 mM calcein in phosphate-buffered saline (PBS, pH 7.4) for CHO cell studies, 20 mM HEPES buffer (pH 7.0) for calcium-release experiments, or 250 mM ammonium sulfate for active loading of vincristine (VCR). Hydration was conducted at either 50 °C or 60 °C in case of VCR preparations, with intermittent vortexing to ensure complete lipid dispersion. The resulting MLV suspensions were extruded through polycarbonate membranes (100 nm pore size) using mini extruder (Avanti Polar Lipids, AL, USA) with 21 passes to obtain large unilamellar vesicles (LUV). Lipid concentrations prior to purification were adjusted to 1.5 mg/mL for PBS- and

Table 1. Annotation of lipid compositions of the investigated liposome samples.

Sample label	Molar ratio			Mass ratio		
	C _{25,25} (mol%)	Egg sphingomyelin (mol%)	Cholesterol (mol%)	C _{25,25} (wt.%)	Egg sphingomyelin (wt.%)	Cholesterol (wt.%)
A100	100	0	0	100	0	0
A0	0	60	40	0	73.4	26.6
A2	2	58.8	39.2	4	70.5	25.5
A5	5	57	38	9.7	66.3	24
A15	15	51	34	26.4	54	19.6
A25	25	45	30	40.4	43.7	15.9
A35	35	39	26	52.3	35	12.7
A45	45	33	22	62.4	27.6	10
SM100	0	100	0	0	100	0

HEPES-buffered liposomes, and 20 mg/mL for VCR-loaded formulations.

Calcium stability assay

LUVs (0.5 mg/mL lipids in 20 mM HEPES, pH 7.0) were incubated with CaCl_2 at final concentrations of 2, 4, 6, and 8 mmol/L. A 5.913 M CaCl_2 stock was used for dosing. Samples were incubated at room temperature for 30 min and then vortexed immediately after CaCl_2 addition to prevent localized concentration gradients. Size and polydispersity index (PDI) were measured by dynamic light scattering (DLS) method using Zetasizer Nano ZS (Malvern Panalytical, UK). EDTA was then added to a final concentration of 40 mM, followed by an additional 30-min incubation and DLS measurement. Each calcium concentration was tested using a freshly prepared sample. Data were analyzed using GraphPad Prism 10.3.1.

Vincristine-loaded liposomes

Two lipid formulations were tested for VCR encapsulation: a control (sphingomyelin:cholesterol, 1.5:1 molar ratio) and a modified formulation containing 2 mol% archaeal lipids. MLV were hydrated in 250 mM ammonium sulfate at 60°C and extruded as described above. Unencapsulated ammonium sulfate was removed by dialysis (MWCO 3 kDa, PBS pH 7.4, four buffer exchanges with an overnight final step). Active loading of VCR was performed by incubating LUVs with VCR sulfate (dissolved in PBS) at 65°C for 15 min followed by 30 min at room temperature. Final concentrations were 0.16 mg/mL VCR and 2.37 mg/mL lipid. Unencapsulated drug was removed by dialysis (MWCO 6–8 kDa, four exchanges in 70-fold PBS volume).

HPLC quantification of VCR encapsulation

The encapsulation efficiency of vincristine was determined using a high-performance liquid chromatography (HPLC) system (Agilent 1260 Infinity, Agilent Technologies, Waldbronn, Germany). Chromatographic separation was performed on a Zorbax Eclipse Plus C18 analytical column (4.6 × 150 mm, 3.5 μm particle size) equipped with an Eclipse XDB-C18 guard column (4.6 × 12.5 mm, 5 μm particle size; Agilent Technologies). The analyte was eluted isocratically using a mobile phase consisting of 33% solvent A (0.1% formic acid in water) and 67% solvent B (acetonitrile containing 0.1% formic acid). The column temperature was maintained at 25°C, the flow rate was set to 1.0 mL/min, and the injection volume was 20 μL. Detection of vincristine in samples was performed using a diode-array detector at 297 nm and compared with the retention time and UV spectra of a standard vincristine solution.

Prior to analysis, all samples were diluted 1:10 in methanol to ensure complete release of the encapsulated compound. The encapsulation efficiency (EE%) was calculated as the ratio between the peak area of the sample signal after dialysis and the peak area of the sample signal before dialysis.

$$EE = \frac{AUC_{encap}}{AUC_{total}} * 100 \quad (1)$$

where AUC_{encap} represents the area under the curve post-dialysis (encapsulated drug) and AUC_{total} represents the total drug content before dialysis.

Chinese hamster ovary (CHO) cell studies

LUVs encapsulating 80 mM calcein in PBS (pH 7.4) were purified by gel filtration using a 20 cm³ Sephadex G-50 column equilibrated with PBS (pH 7.4). All calcein-loaded liposomes were sterile-filtered through 0.20-μm pore size membranes and used within 24 h. Purified liposomes were stored at 4°C in the dark. Morphological parameters of liposomes were assessed by DLS (Appendix 3). To minimize calcein contamination, glassware and plasticware were cleaned with 1 M NaOH where applicable.

Chinese hamster ovary (CHO-K1) (source: #85051005 ECACC) were cultured in HAM F-12 with 9.1% fetal bovine serum, 910 U/L penicillin, 0.91 mg/L streptomycin, and 45.5 mg/L gentamycin. Cells were maintained in a humidified atmosphere at 37°C and 5% CO₂. Following trypsinization and cell counting via hemocytometer, the required transfer volume was calculated using:

$$V_c = \frac{N_c}{C_c} \quad (2)$$

where V_c is the transfer volume, N_c the desired cell number, and C_c the measured cell concentration. Cells were maintained at 37°C with 5% CO₂.

For flow cytometry analysis, CHO cells (4×10^6 cells/mL) were mixed with liposomal colloidal suspension in PBS (0.08 mg/mL lipid) to obtain final concentrations of 1×10^6 cells/mL and 0.02 mg/mL lipid. Cells were incubated at 37°C with 5% CO₂, and gently vortexed every 30 min to minimize adhesion to tube walls. Calcein fluorescence was measured at 10, 30, 60, 120, and 180 min with 488 nm blue laser using 530/30 nm band-pass filter on Attune NxT flow cytometer (Thermo Fisher Scientific, USA). Data acquisition and analysis were performed using Attune NxT software. In gating process, cellular debris and aggregates were excluded from analysis using forward scatter/side scatter (FSC/SSC) gating. The median fluorescence intensity (MFI) of calcein was obtained from the fluorescence intensity histogram and corresponds to the median value of the measured signal.

For fluorescence microscopy, 300 μL of the previously prepared mixture (final concentrations: 0.02 mg/mL lipids and 1×10^6 cells/mL) was added to a mini Petri dish containing 1.5 mL HAM-F12 medium supplemented with 9.1% FBS. Cells were incubated for 24 h at 37°C in a humidified atmosphere with 5% CO₂. Imaging was performed at 10x and 40x magnification using inverted microscope Leica DM IL LED (Leica, Germany). Microscope illumination was set to 82% brightness, and the gamma value was adjusted to 0.89. Fluorescence micrographs were acquired immediately after opening the fluorescence shutter to minimize calcein bleaching. All image acquisition settings were kept

constant across samples. Calcein fluorescence was excited using a blue BG38 filter, with the light source intensity set to maximum. Images were processed in Fiji (ImageJ). The mean fluorescence intensity per pixel F_{mean} was calculated to quantify cellular fluorescence from micrographs. This was determined using the total fluorescence intensity of the image F_{max} expressed in arbitrary units, a.u.), defined as the sum of fluorescence values of all pixels, and the total number of pixels in the image N_{pixel} . Background signal was accounted for by subtracting the minimum pixel intensity F_{min} (a.u.), corresponding to background fluorescence. The final formula used was:

$$F_{\text{mean}} = \left(\frac{F_{\text{max}}}{N_{\text{pixel}}} \right) - F_{\text{min}} \quad (3)$$

Results

Effect of calcium ions on liposome morphology

Calcium ions are known to significantly influence the structural integrity of liposomal membranes. Their effect is largely lipid-dependent, especially in systems containing phosphatidylcholine (PC). Previous studies have shown that Ca^{2+} ions can interact with phosphate groups of PC headgroups, reducing electrostatic repulsion and promoting liposome aggregation and fusion [13]. These interactions lead to the formation of larger vesicles through fusion of smaller ones, as demonstrated by light scattering, fluorescence resonance energy transfer (FRET), and electron microscopy.

In contrast, liposomes composed of glycolipids, e.g. digalactosyldiacylglycerol and sulfoquinovosyldiacylglycerol, exhibit higher structural integrity. Hinch (2003) [14] reported that although calcium ions induce dehydration of the interfacial region and promote hydrogen bonding between glycosidic headgroups, these liposomes remain intact, without evidence of membrane fusion or content leakage.

The destabilizing effects of calcium are more pronounced in liposomes containing negatively charged lipids like phosphatidylglycerol, where Ca^{2+} promotes fusion and leakage. This is particularly relevant when examining archaeal $\text{C}_{25,25}$ lipid-based vesicles, which typically exhibit high negative surface charges (zeta potential ~ -50 mV). Despite this, archaeal lipids possess one or two bulky glycosylated polar headgroups (e.g. glucose or inositol-glucose) that introduce steric hindrance, potentially inhibiting calcium-induced aggregation and fusion. Additionally, their isoprenoid chains are highly methylated and interdigitated, forming a zipper-like structure that may enhance membrane rigidity and stability.

To investigate this further, we evaluated liposomes composed of varying molar ratios of archaeal lipids ($\text{C}_{25,25}$) mixed with sphingomyelin (SM) and cholesterol (CH). The goal was to determine whether an optimal combination exists in which the beneficial properties of each component are retained while minimizing destabilizing effects in the presence of calcium.

Among the tested formulations, the sample designated A35 (35 mol% archaeal lipids) showed the greatest stability. Upon exposure to 6 mM Ca^{2+} , both the average hydrodynamic diameter and polydispersity index (PDI) remained largely unchanged and reversible upon treatment with 40 mM EDTA (Figures 2 and 3). The pure archaeal lipid system (A100) exhibited calcium-induced destabilization only at 8 mM Ca^{2+} and similarly responded to EDTA reversal. This suggests that at lower concentrations, calcium is insufficient to fully engage all available phosphate sites on archaeal lipid headgroups.

Conversely, formulations A15 and A25 (15 and 25 mol% archaeal lipids, respectively) underwent complete destabilization at just 2 mM Ca^{2+} , exhibiting high PDI values (~ 1.0) and reduced size (< 500 nm). These results suggest that formulations with low archaeal content may lack sufficient negatively charged headgroups to support inter-vesicle cross-linking. In contrast, formulations with higher archaeal content may offer too many binding sites relative to the calcium present,

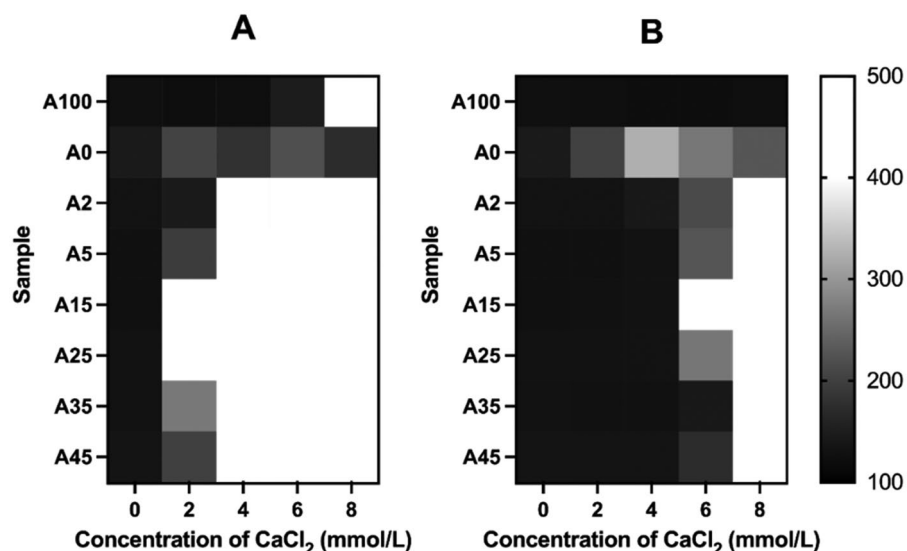


Figure 2. Heat maps illustrate the effect of CaCl_2 concentration on LUV mean diameter after 30 min at room temperature (A) and after subsequent addition of 40 mM EDTA (B). LUVs consisted of 100% archaeal lipids (A100) or SM:CH (1.5:1 molar ratio) with varying archaeal lipid content of 0–45 mol% (A0–A45).

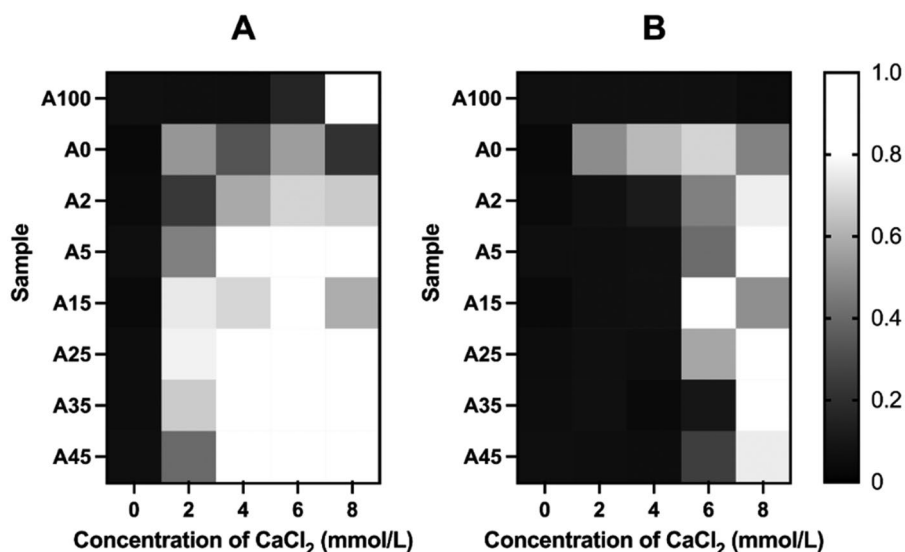


Figure 3. Heat maps illustrate the effect of CaCl₂ concentration on LUV polydispersity index (PDI) after 30 min at room temperature (A) and after subsequent addition of 40 mM EDTA (B). LUVs consisted of 100% archaeal lipids (A100) or SM:CH (1.5:1 molar ratio) with varying archaeal lipid content of 0–45 mol% (A0–A45).

reducing the probability of effective vesicle bridging at lower Ca²⁺ concentrations.

Stability at 2 mM Ca²⁺ is particularly relevant, as it closely approximates physiological calcium concentrations in adult human blood (1.22 ± 0.07 mM) [15]. The A2 formulation, containing 2 mol% archaeal lipids (C_{25,25}), remained stable at this concentration even before EDTA treatment. Notably, it was the only C_{25,25}-containing formulation that did not exceed a PDI value of 1.0 at any tested Ca²⁺ concentration. This high colloidal stability is attributed to a sufficiently low zeta potential, which offsets the anionic character of the formulation.

The binary SM:CH mixture (A0) exhibited only modest changes in morphological parameters upon Ca²⁺ exposure, suggesting limited aggregation compared to archaeal-containing formulations (Figures 2 and 3). However, these changes were irreversible after the addition of 40 mM EDTA, indicating calcium-induced fusion. This behavior is consistent with the zwitterionic nature of phosphatidylcholine headgroups, which have lower calcium affinity than negatively charged glycosylated archaeal heads. While the degree of aggregation is reduced, fusion still occurs, most likely because the choline group provides less steric hindrance than the bulkier glycosidic groups present in archaeal lipids.

Despite their strong anionic surface charge, archaeal lipid-rich liposomes did not undergo fusion at Ca²⁺ concentrations up to 4–6 mM. This is critical for drug delivery system design, as inter-vesicle fusion can lead to premature release of encapsulated agents. The full reversibility of liposome size and PDI following EDTA treatment suggests that drug retention remains unaffected by transient calcium-induced aggregation.

Together, these findings highlight the importance of lipid composition in determining calcium sensitivity. Specifically, they support the hypothesis that archaeal lipids, due to their unique structural and chemical features, confer enhanced resistance to calcium-induced destabilization, particularly when used at optimized intermediate concentrations.

Encapsulation efficiency (EE) of active vincristine loading

In addition to liposome stability, high encapsulation efficiency (EE) is a key parameter in the development of liposomal drug delivery systems. Efficient loading is particularly challenging in liposomes ranging from 50 to 150 nm mean size due to their limited internal volume. Active loading exploits a transmembrane gradient that converts the drug from a membrane-permeable to an impermeable form after encapsulation [16]. This approach typically requires high lipid concentrations to facilitate drug permeation across the bilayer.

Liposomes composed entirely of archaeal lipids from *A. pernix* may hinder active loading due to their unique bilayer properties. Gmajner et al. (2011) [6] demonstrated that archaeal bilayers are impermeable to calcein. Additionally, at acidic pH (≤ 4.0), these liposomes lose structural integrity and release their contents (Gmajner et al., 2011b) [17]. Since active loading depends on the establishment of a steep internal pH gradient, which can reach values as low as pH ~ 2.7 following ammonium sulfate-based loading [16], liposomes composed entirely of archaeal lipids (100 mol%) are likely unsuitable for this method.

In prior work, we identified the SM:CH formulation with 2 mol% C_{25,25} archaeal lipids as exhibiting favorable physicochemical stability in biological conditions. We therefore investigated whether this low level of archaeal incorporation interferes with active loading efficiency. Previous studies and commercial formulations have shown that SM:CH-based systems achieve high EE values ranging from 89% to 97% when actively loaded with vincristine [18]. In our study, SM:CH control formulation (A0) achieved an EE of $87.9 \pm 1.5\%$ (Table 2), slightly lower than literature values but consistent with effective active loading.

The relatively low encapsulation efficiency (EE) of the control formulation (A0) is likely a consequence of its morphological characteristics, specifically its larger average hydrodynamic

Table 2. Encapsulation efficiency of LUVs loaded with vincristine sulfate was evaluated using the ammonium sulfate gradient method.

$C_{25,25}$ (mol%)	EE (%)	After active loading			After dialysis		
		Determined concentration ($\mu\text{g/L}$)	Mean diameter (nm)	PDI	Determined concentration ($\mu\text{g/L}$)	Mean diameter (nm)	PDI
0 (A0)	87.9 ± 1.5	163.7 ± 2.3	152 ± 55	0.186	143.9 ± 0.3	153 ± 59	0.174
2 (A2)	95.2 ± 0.4	158.2 ± 3.8	118 ± 40	0.080	150.7 ± 4.3	120 ± 45	0.092

Average diameter and PDI were measured, and VCR concentration was quantified by HPLC, both immediately after active loading and after dialysis to remove unencapsulated drug.

diameter and higher polydispersity index (PDI), as determined by dynamic light scattering (DLS). These properties may arise from the absence of co-solvents such as ethanol during extrusion-based LUV preparation. Ethanol is known to reduce the mean liposome size and increase polydispersity by increasing the area per lipid molecule and decreasing the membrane bending modulus, among other effects [19].

Additionally, the pronounced effect of $C_{25,25}$ archaeal lipids on LUV mean diameter could be attributed to the substantially higher lipid concentration used during extrusion (20 mg/mL) compared to other analyses (1.5 mg/mL). This difference in formulation conditions resulted in a reduction in mean liposome size from 152 nm to 118 nm. Extrusion constrains vesicle size through mechanically driven deformation and resealing processes [20]. In the presence of cholesterol, the extrusion force increases with lipid concentration [21], which can influence vesicle formation in complex systems such as $C_{25,25}$ /SM/CH. In our previous work [9], the addition of 2 mol% $C_{25,25}$ lipids enabled the formation of small unilamellar vesicles during sonication and reduced the membrane fluidity of SM/CH formulations. Given the pronounced effects observed during sonication, similar effects may also occur during extrusion, particularly at higher lipid concentrations.

Using the formulation containing 2 mol% $C_{25,25}$ (A2), an encapsulation efficiency of $95 \pm 0.4\%$ was achieved, which is comparable to values reported for clinically approved liposomal drugs such as Doxil and Marqibo [18,22]. Corresponding chromatograms are provided in appendices 4A and 4B. DLS analysis revealed that A2 liposomes exhibited a smaller average diameter and lower PDI than the control A0, which may account for the observed difference in EE.

As the active loading protocol was adapted from the Marqibo procedure, which involves a relatively short encapsulation time, it is plausible that the A0 sample did not achieve optimal loading efficiency due to its larger vesicle size relative to liposomes in Marqibo (approximately 100 nm). In contrast, the smaller size and higher surface-to-volume ratio of A2 liposomes likely facilitated more efficient drug loading within the same 15-min incubation period.

The high EE observed for A2 also suggests that the physicochemical properties of *A. pernix* archaeal lipids do not interfere with active loading when present at low concentrations. This was further confirmed by HPLC-based quantification of VCR. Both A0 and A2 samples were prepared with an initial vincristine concentration of 160 $\mu\text{g/mL}$, matching that of the commercial formulation Marqibo. The measured pre-dialysis VCR concentrations showed no significant deviation from the theoretical values (Table 2), indicating no loss or degradation of the drug during the active loading process in either formulation.

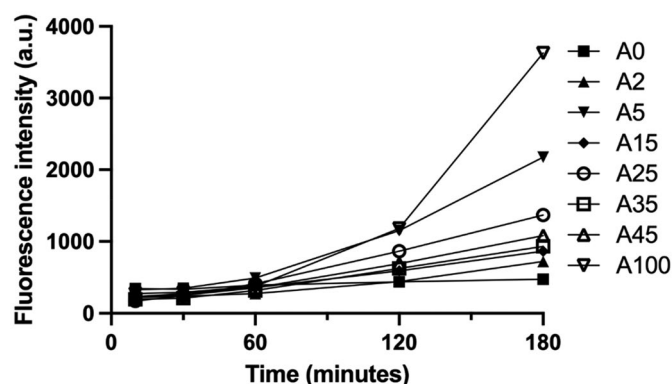


Figure 4. Fluorescence intensity of encapsulated calcein in LUV samples was measured by flow cytometry after 10-, 30-, 60-, 120-, and 180-min incubation with CHO cells at 37°C. Liposomes included 100% archaeal lipids (A100) and SM:CH mixtures (1.5:1 molar ratio) with 0–45 mol% archaeal lipid content (A0–A45).

Liposome interactions with CHO cells

Flow cytometry

The lipid composition of liposomes, including surface charge and bilayer structure, plays a critical role in determining *in vitro* stability and drug release kinetics in biological systems. Liposome stability in medium is directly associated with enhanced cellular uptake and sustained, controlled drug release [23]. Therefore, optimizing lipid composition is essential to improve the therapeutic potential of lipid-based drug delivery systems.

Markelc et al. (2015) [8] demonstrated that liposomes composed of 100 mol% $C_{25,25}$ archaeal lipids rapidly aggregate and release their contents within minutes, making them unsuitable for drug delivery strategies that rely on the enhanced permeability and retention (EPR) effect. Consistent with these findings, our study showed that the $C_{25,25}$ -only formulation exhibited the lowest stability among all tested samples, as indicated by the highest increase in calcein fluorescence signal (3627) following 180 min of incubation with CHO cells (Figure 4).

In contrast, the SM:CH binary mixture demonstrated the highest stability, with the lowest calcein fluorescence intensity (474 a.u.) under the same conditions. These results confirm the *in vitro* stability of SM:CH-based liposomes, in agreement with previously published data on this delivery system [24,25].

For formulations containing various fractions of $C_{25,25}$ mixed with SM:CH, slightly reduced stability was observed compared to the pure SM:CH formulation (A0) (Figure 4). However, the sample with 2 mol% $C_{25,25}$ (A2) showed only a modest increase in calcein fluorescence relative to A0, with noticeable differences emerging only after 180 min of incubation. In contrast, the 5 mol% $C_{25,25}$ sample (A5) displayed the highest release of

fluorescence among all mixed formulations, indicating the greatest extent of calcein release. This destabilization observed in A5 remains difficult to explain, although similar results were confirmed by fluorescence microscopy.

Further increases in the $C_{25,25}$ content (A15, A25, A35, and A45) led to a slight reduction in stability relative to A2, although the differences between these higher-percentage formulations were not pronounced. These findings suggest that increasing the concentration of archaeal lipids impacts liposome stability, though the effect does not follow a clear or linear trend at higher inclusion levels.

As previously demonstrated by quantitative analysis of median fluorescence intensity using the 530/30nm bandpass filter, visual inspection also confirms that the SM:CH (A0) formulation and the 2 mol% $C_{25,25}$ formulation (A2) exhibit the highest stability, as evidenced by the lowest increase in fluorescence signal (Appendix 5). In earlier serum stability studies, we observed that liposome-cell interactions are most pronounced within the first few minutes of exposure, corresponding to the greatest release of calcein [9]. However, due to the technical limitations of flow cytometry, immediate measurement at time zero ($t=0$) could not be performed.

In $C_{25,25}$:SM:CH formulations containing 5–45 mol% $C_{25,25}$ (A5–A45), a small subpopulation of CHO cells exhibited stronger fluorescence signals (10^4 – 10^5), i.e., observed as a secondary peak in fluorescence histogram (Appendix 5). This effect was not observed in samples with 100 mol% $C_{25,25}$ (A100), the SM:CH binary system (A0), or the 2 mol% $C_{25,25}$ formulation (A2). While this increase could suggest uptake of liposomes followed by intracellular release of calcein, fluorescence microscopy (Figure 5) did not support this hypothesis, as no localized increase in fluorescence was detected within individual CHO cells. Furthermore, this signal cannot be attributed to lipid aggregates, as such aggregates were detected only in the A100 formulation. Since flow cytometry analyzes individual cells and does not detect particles below a certain size (detection is limited to $0.5\mu\text{m}$) or with non-cell-like scattering properties, the observed fluorescence increase is unlikely to result from the presence of aggregates. This unusual observation warrants further investigation to elucidate the mechanism underlying the elevated fluorescence in specific cell subpopulations.

Across all samples, CHO cell morphology remained unaffected based on event scatter of FSC/SSC dot plot. This indicates that none of the tested formulations had a substantial negative impact on cell integrity or viability. These findings support the general biocompatibility of the investigated systems and are consistent with previous reports by Napotnik et al. (2013) [7], who demonstrated high CHO cell compatibility with 100 mol% $C_{25,25}$ liposomes. The lack of cytotoxicity in $C_{25,25}$:SM:CH formulations is expected, given the reduced content of archaeal lipids in favor of conventional membrane lipids as the components are naturally found in human cell membranes [26], which are inherently non-cytotoxic. These results further confirm the suitability of such formulations for biomedical applications.

No increase in fluorescence was observed within individual CHO cells for any formulation, indicating that calcein was not delivered via direct membrane fusion. If liposomes were internalized, e.g., through pinocytosis, they remained intact within the cells, as no intracellular fluorescent signal was

detected. This observation is consistent with Napotnik et al. (2013) [7], who reported minimal fusion of 100 mol% $C_{25,25}$ liposomes with CHO cells, particularly when compared to other cell lines such as EA.hy926.

Fluorescence microscopy

Following incubation of CHO cells with the 100 mol% $C_{25,25}$ formulation (A100), bright fluorescent patches were observed under fluorescence microscopy (Figure 5). This phenomenon was unique to A100. Quantification confirmed the highest maximal fluorescence intensity for this sample (249), in contrast to the average signal of 147 ± 3 observed for mixed formulations (Table 3). Similar bright fluorescent areas resulting from calcein-loaded archaeosomes have been described previously by Napotnik et al. (2013) [7] in *in vitro* cell studies, and by Markelc et al. (2015) [8] in *in vivo* experiments in mice.

Fluorescent patches of the A100 formulation are presumed to be lipid aggregates formed due to instability of pure $C_{25,25}$ archaeosomes in biological environments. The localized, high fluorescence intensity suggests that calcein dilution occurred, disrupting self-quenching and thus increasing signal intensity. The observable size of these patches under light microscopy indicates that they do not originate from individual liposomes (~ 120 nm), which are below the resolution limit of standard optical microscopy.

The highest average fluorescence signals were recorded for the A100 and A15 formulations, at 23.6 and 20.9, respectively (Table 3). The increased permeability of A100 was further confirmed by flow cytometry, which also showed elevated calcein signal relative to other samples. Among the mixed formulations, A15 exhibited the lowest stability, consistent with results from previous serum stability assays and with its highest aggregation propensity in the presence of calcium.

Conversely, the lowest average fluorescence was observed for the binary SM:CH mixture (A0) and the 2 mol% $C_{25,25}$ formulation (A2), with values of 6.9 and 6.2, respectively. The *in vitro* stability of SM:CH is well documented, including in *in vivo* settings [25]. A2 exhibited a similar average signal, suggesting that incorporation of 2 mol% $C_{25,25}$ does not compromise the stability of the SM:CH system under CHO cell culture conditions (HAM F-12 medium). This was further confirmed by the addition of detergent, which caused complete calcein release and a sharp increase in fluorescence intensity (Appendix 6). Nevertheless, even low levels of $C_{25,25}$ significantly influence physicochemical properties such as morphology and zeta potential, as confirmed by previous studies [9].

In contrast, formulations with ≥ 5 mol% $C_{25,25}$ consistently showed increased average fluorescence values calculated from micrographs, exceeding those of both the pure SM:CH system and the 2 mol% $C_{25,25}$ sample. These results indicate a concentration-dependent effect of $C_{25,25}$ lipids, where higher content leads to reduced *in vitro* stability, an effect already demonstrated in the fully archaeal system (A100) [9].

For the CHO cell interaction studies, we used HAM F-12 culture medium supplemented with 9.1% FBS. According to manufacturer specifications, this medium contains calcium at concentrations between 0.546 and 0.590 mM. In prior stability studies, we demonstrated that liposomal formulations

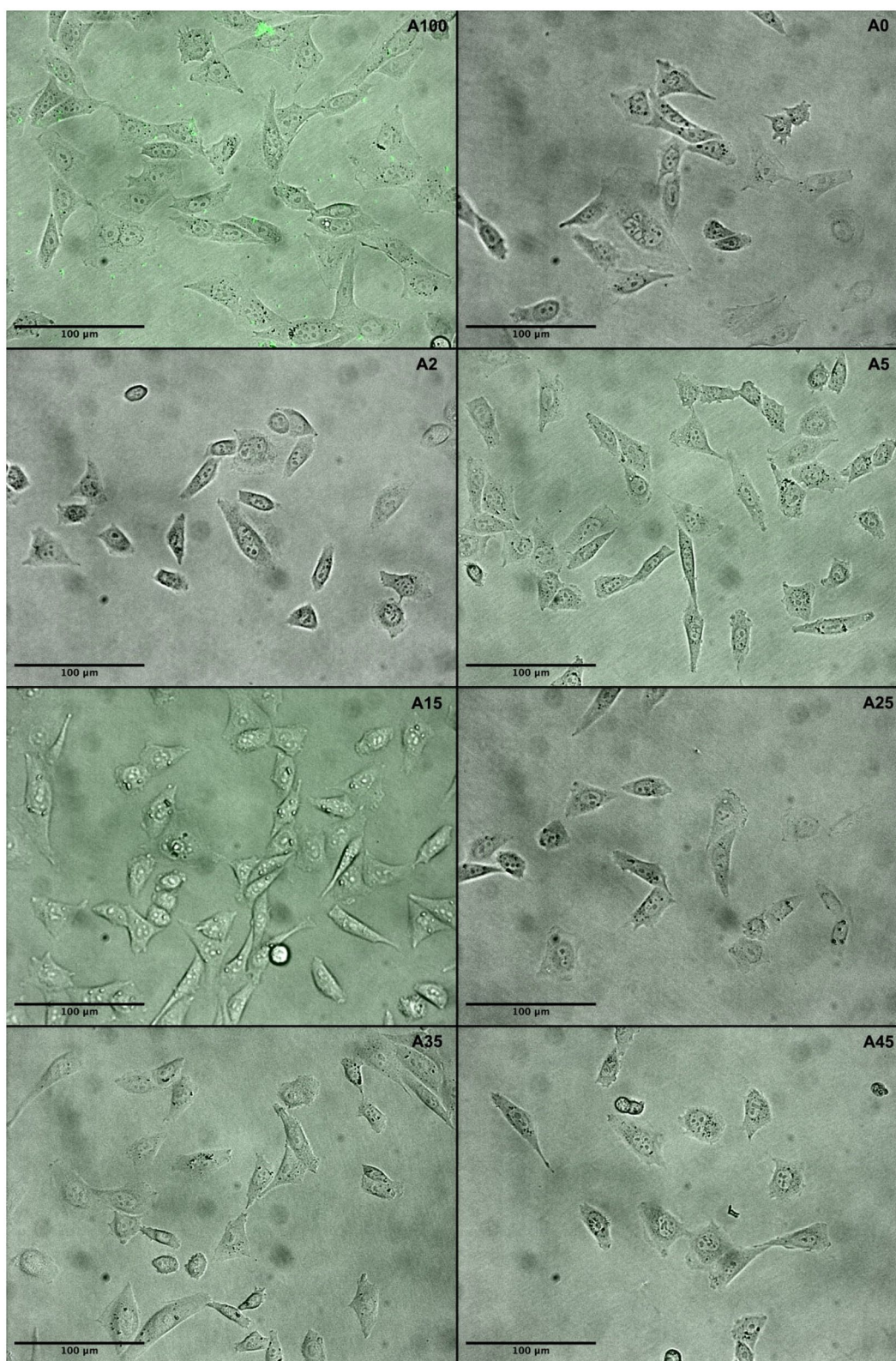


Figure 5. Fluorescence micrographs of CHO cells after 24 h incubation at 37°C with LUVs containing calcein. Liposomes were composed of 100% archaeal lipids (A100) or SM:CH (constant molar ratio 1.5:1) with 0–45 mol% archaeal lipid content (A0–A45).

containing 15 and 25 mol% $C_{25,25}$ underwent calcium-induced destabilization at 2 mM Ca^{2+} , which was reversible upon EDTA addition (see section Effect of Calcium Ions on Liposome Morphology). Based on these findings, we conclude that the calcium ion concentration in the culture medium is not the primary cause of calcein release observed in the fluorescence micrographs.

Discussion

Our results demonstrate that liposomes composed of pure archaeal lipids and SM:CH mixtures with varying $C_{25,25}$ content exhibit stabilization patterns reminiscent of those observed with glycolipids. Isoprenoid chains of $C_{25,25}$ archaeal lipids may potentially intercalate with the acyl chains of sphingomyelin

Table 3. Quantified maximum and average calcein fluorescence values calculated from fluorescence micrographs of CHO cells after 24 h incubation at 37°C with various LUV formulations.

Sample label	Max fluorescence signal (a.u.)	Mean fluorescence signal (a.u.)
A100	249	23.6
A0	143	6.9
A2	143	6.2
A5	150	16.5
A15	151	20.9
A25	144	9.6
A35	148	14.1
A45	145	11.6

Liposomes consisted of 100% archaeal lipids (A100) or SM:CH (constant molar ratio 1.5:1) with 0–45 mol% archaeal lipid content (A0–A45).

(SM) enriched with cholesterol (CH), similar to observations reported for glycolipids [27]. Upon addition of calcium ions, DLS analysis revealed significant increases in average diameter and PDI for $C_{25,25}$:SM:CH formulations, indicating destabilization relative to the binary SM:CH mixture. However, this effect was almost entirely reversible with 40 mM EDTA at calcium concentrations up to 4 mM, suggesting that the destabilization was primarily due to liposome aggregation rather than fusion. Post-EDTA DLS profiles were nearly identical to pre-calcium measurements, confirming reversible aggregation and supporting the notion that $C_{25,25}$ lipids contribute stabilizing effects analogous to glycolipids [27].

The incorporation of SM and CH further improves the safety profile of these systems, as both are natural components of cell membranes and are unlikely to disrupt membrane function. Notably, SM is degradable by acid sphingomyelinase, which is localized in lysosomes [28], potentially enabling controlled drug release following endocytotic uptake of intact liposomes.

Several studies have highlighted the potential of archaeosomes as vaccine delivery platforms, largely due to their potent adjuvant properties. These effects are typically achieved using semi-synthetic lipids derived from archaeol that induce strong immune responses [29]. However, these vaccine formulations require blends of negatively and neutrally charged glycolipids to produce homogeneous and stable vesicles, and their synthesis often involves complex procedures [30]. Our findings suggest that $C_{25,25}$:SM:CH formulations interact with proteins in biological media, which we attribute to the presence of $C_{25,25}$ lipids. Specifically, we observed pronounced calcein leakage from liposomes containing 15 mol% $C_{25,25}$ in an SM:CH mixture (1.5:1 molar ratio) during serum incubation, indicating that $C_{25,25}$ may contribute to immune activation. Nonetheless, further immunological studies are needed to fully assess their adjuvant potential. Zavec et al. (2014) [31] demonstrated that the sugar moieties on $C_{25,25}$ lipid headgroups can interact with listeriolysin O in the absence of CH, which is typically required for protein-membrane interactions. Similarly, Krishnan et al. (2000) [32] reported immune activation by various archaeal lipids, despite the structural differences between their headgroups and those of $C_{25,25}$ lipids.

Our formulations containing SM:CH: $C_{25,25}$ displayed variable stability depending on the $C_{25,25}$ content. A possible explanation

for the destabilization observed *in vitro*, particularly at 15 mol% $C_{25,25}$, is the relatively large size of the polar headgroups compared with those of SM, which may influence surface exposure in a concentration-dependent manner. At higher proportions (≥ 25 mol%), stability appears to improve again, likely due to increased lateral steric hindrance from the densely packed headgroups. These findings suggest that the effect of $C_{25,25}$ on stability is nonlinear and merit further exploration, particularly in the context of adjuvant activity.

Despite their promising properties, liposomes composed entirely of archaeal lipids are unlikely to be commercially viable for drug delivery due to the extreme growth conditions of archaea (e.g., high temperatures) and the complexity of lipid extraction and purification. Moreover, archaeal lipid composition can vary significantly even within species, depending on environmental conditions. As a result, recent efforts have focused on the development of synthetic and semi-synthetic analogues that bypass the need for archaeal cultivation [5]. Another strategy involves combining archaeal lipids with conventional phospholipids such as egg phosphatidylcholine, with the aim of retaining the stabilizing benefits [17]. Understanding the structural determinants of lipid behavior in archaeal membranes remains essential for formulation design.

Ultimately, predicting the behavior of mixed lipid systems is inherently challenging and requires systematic characterization to identify optimal compositions for pharmaceutical applications. Van Uiter et al. (2010) [33] demonstrated that the stability of binary lipid mixtures is not linearly related to composition, underscoring the need for detailed experimental validation. This is particularly critical in complex systems such as lipid nanoparticles, where the interplay between formulation components and biological environments makes predictive modeling nearly impossible. Even for relatively well-established systems like liposomal drugs, development remains nontrivial, which is highlighted by the fact that it took three years after the Doxil patent expired for a comparable generic (LipoDox) to reach the market [34].

Given the relatively straightforward aerobic cultivation of *A. pernix* K1, $C_{25,25}$:SM:CH liposomes may represent an economically feasible advanced drug delivery platform. It is important to note that many studies report archaeal lipid content in mol%, which can be misleading due to the significantly higher molecular weight of archaeal lipids compared to conventional ones. This is especially true for tetraether lipids such as caldarchaeols, whose molecular weights can be 3–4 times greater than those of standard phospholipids.

Disclosure statement

The authors declare that the research was conducted in the absence of any commercial or financial relationships that could be construed as a potential conflict of interest.

Funding

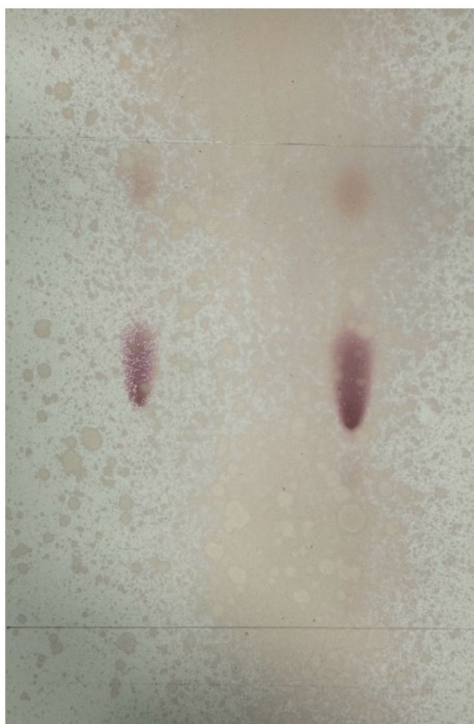
This research was funded by Slovenian Research Agency (P4-0121).

References

- [1] Ahmed KS, Hussein SA, Ali AH, et al. Liposome: Composition, characterisation, preparation, and recent innovation in clinical applications. *J Drug Target*. 2019;27(7):742–761. doi: [10.1080/1061186X.2018.1527337](https://doi.org/10.1080/1061186X.2018.1527337).
- [2] Rothschild LJ, Mancinelli RL. Life in extreme environments. *Nature*. 2001;409(6823):1092–1101. doi: [10.1038/35059215](https://doi.org/10.1038/35059215).
- [3] Jacquemet A, Barbeau J, Lemiègre L, et al. Archaeal tetraether bipolar lipids: structures, functions and applications. *Biochimie*. 2009;91(6):711–717. doi: [10.1016/j.biochi.2009.01.006](https://doi.org/10.1016/j.biochi.2009.01.006).
- [4] Patel GB, Sprott GD. Archaeobacterial ether lipid liposomes (archaeosomes) as novel vaccine and drug delivery systems. *Crit Rev Biotechnol*. 1999;19(4):317–357. doi: [10.1080/0738-859991229170](https://doi.org/10.1080/0738-859991229170).
- [5] Benvegna T, Lemiègre L, Cammas-Marion S. New generation of liposomes called archaeosomes based on natural or synthetic archaeal lipids as innovative formulations for drug delivery. *Recent Pat Drug Deliv Formul*. 2009;3(3):206–220. doi: [10.2174/187221109789105630](https://doi.org/10.2174/187221109789105630).
- [6] Gmajner D, Ota A, Šentjerc M, et al. Stability of diether C25,25 liposomes from the hyperthermophilic archaeon *Aeropyrum Pernix* K1. *Chem Phys Lipids*. 2011;164(3):236–245. doi: [10.1016/j.chemphyslip.2011.01.005](https://doi.org/10.1016/j.chemphyslip.2011.01.005).
- [7] Napotnik TB, Valant J, Gmajner D, et al. Cytotoxicity and uptake of archaeosomes prepared from *Aeropyrum Pernix* lipids. *Hum Exp Toxicol*. 2013;32(9):950–959. doi: [10.1177/0960327113477875](https://doi.org/10.1177/0960327113477875).
- [8] Markelc B, Napotnik TB, Ota A, et al. Archaeosomes prepared from *Aeropyrum Pernix* K1 lipids as an in vivo targeted delivery system for subsequent nanosecond electroporation. In *6th European Conference of the International Federation for Medical and Biological Engineering*; Lacković, I., Vasić, D., Eds.; IFMBE Proceedings; Springer International Publishing: Cham, 2015; Vol. 45, pp 561–564. doi: [10.1007/978-3-319-11128-5_140](https://doi.org/10.1007/978-3-319-11128-5_140).
- [9] Kejžar J, Mrak P, Osojnik Črnivec IG, et al. Influence of archaeal lipids isolated from *Aeropyrum Pernix* K1 on physicochemical properties of sphingomyelin-cholesterol liposomes. *Biochim Biophys Acta Biomembr*. 2024;1866(7):184374. doi: [10.1016/j.bbamem.2024.184374](https://doi.org/10.1016/j.bbamem.2024.184374).
- [10] Milek I, Cigic B, Skrt M, et al. Optimization of growth for the hyperthermophilic archaeon *Aeropyrum Pernix* on a small-batch scale. *Can J Microbiol*. 2005;51(9):805–809. doi: [10.1139/w05-060](https://doi.org/10.1139/w05-060).
- [11] Morii H, Yagi H, Akutsu H, et al. A novel phosphoglycolipid archae-tidyl(glucosyl)inositol with two sesterterpanyl chains from the aerobic hyperthermophilic archaeon *Aeropyrum Pernix* K1. *Biochim Biophys Acta*. 1999;1436(3):426–436. doi: [10.1016/S0005-2760\(98\)00157-X](https://doi.org/10.1016/S0005-2760(98)00157-X).
- [12] Ota A, Gmajner D, Šentjerc M, et al. Effect of growth medium pH of *Aeropyrum Pernix* on structural properties and fluidity of archaeosomes. *Archaea*. 2012;2012:285152–285159. doi: [10.1155/2012/285152](https://doi.org/10.1155/2012/285152).
- [13] Tarahovsky YS, Yagolnik EA, Muzafarov EN, et al. Calcium-Dependent aggregation and fusion of phosphatidylcholine liposomes induced by complexes of flavonoids with divalent iron. *Biochim Biophys Acta*. 2012;1818(3):695–702. doi: [10.1016/j.bbamem.2011.12.001](https://doi.org/10.1016/j.bbamem.2011.12.001).
- [14] Hincha DK. Effects of calcium-induced aggregation on the physical stability of liposomes containing plant glycolipids. *Biochim Biophys Acta*. 2003;1611(1-2):180–186. (doi: [10.1016/S0005-2736\(03\)00053-1](https://doi.org/10.1016/S0005-2736(03)00053-1)).
- [15] Fogh-Andersen N, Christiansen TF, Komarmy L, et al. Measurement of free calcium ion in capillary blood and serum. *Clin Chem*. 1978;24(9):1545–1552. doi: [10.1093/clinchem/24.9.1545](https://doi.org/10.1093/clinchem/24.9.1545).
- [16] Tazina EV, Kostin KV, Oborotova NA. Specific features of drug encapsulation in liposomes (a review). *Pharm Chem J*. 2011;45(8):481–490. doi: [10.1007/s11094-011-0661-4](https://doi.org/10.1007/s11094-011-0661-4).
- [17] Gmajner D, Grabnar PA, Znidarič MT, et al. Structural characterization of liposomes made of diether archaeal lipids and Dipalmitoyl-L- α -phosphatidylcholine. *Biophys Chem*. 2011;158(2-3):150–156. doi: [10.1016/j.bpc.2011.06.014](https://doi.org/10.1016/j.bpc.2011.06.014).
- [18] Monte W, Abra R, Luo B, et al. A Ready-to-Use Formulation for Vincristine Sulfate Liposome Injection, January 26, 2017. <https://patentscope.wipo.int/search/en/detail.jsf?docId=WO2017015584>. (accessed 2024-11-27).
- [19] Pal A, Sunthar P, Khakhar DV. Effects of ethanol addition on the size distribution of liposome suspensions in water. *Ind Eng Chem Res*. 2019;58(18):7511–7519. doi: [10.1021/acs.iecr.8b05028](https://doi.org/10.1021/acs.iecr.8b05028).
- [20] Mayer LD, Hope MJ, Cullis PR. Vesicles of variable sizes produced by a rapid extrusion procedure. *Biochim Biophys Acta*. 1986;858(1):161–168. doi: [10.1016/0005-2736\(86\)90302-0](https://doi.org/10.1016/0005-2736(86)90302-0).
- [21] Dosekoc J, Dałek P, Przybyło M, et al. The elucidation of the molecular mechanism of the extrusion process. *Materials (Basel)*. 2021;14(15):4278. doi: [10.3390/ma14154278](https://doi.org/10.3390/ma14154278).
- [22] Barenholz Y. Doxil®—the first FDA-approved nano-drug: lessons learned. *J Control Release*. 2012;160(2):117–134. doi: [10.1016/j.jconrel.2012.03.020](https://doi.org/10.1016/j.jconrel.2012.03.020).
- [23] Yang K, Tran K, Salvati A. Tuning liposome stability in biological environments and intracellular drug release kinetics. *Biomolecules*. 2022;13(1):59. doi: [10.3390/biom13010059](https://doi.org/10.3390/biom13010059).
- [24] Semple SC, Leone R, Wang J, et al. Optimization and characterization of a sphingomyelin/cholesterol liposome formulation of vinorelbine with promising antitumor activity. *J Pharm Sci*. 2005;94(5):1024–1038. doi: [10.1002/jps.20332](https://doi.org/10.1002/jps.20332).
- [25] Webb M, Harasym T, Masin D, et al. Sphingomyelin-cholesterol liposomes significantly enhance the pharmacokinetic and therapeutic properties of vincristine in murine and human tumour models. *Br J Cancer*. 1995;72(4):896–904. doi: [10.1038/bjc.1995.430](https://doi.org/10.1038/bjc.1995.430).
- [26] Slotte JP. Sphingomyelin-cholesterol interactions in biological and model membranes. *Chem Phys Lipids*. 1999;102(1-2):13–27. doi: [10.1016/S0009-3084\(99\)00071-7](https://doi.org/10.1016/S0009-3084(99)00071-7).
- [27] Rog T, Orłowski A, Manna M, et al. Cholesterol modulated interdigitation of long-chain sphingomyelin and glycolipids. *Biophys J*. 2016;110(3):578a–579a. doi: [10.1016/j.bpj.2015.11.3094](https://doi.org/10.1016/j.bpj.2015.11.3094).
- [28] Jenkins RW, Canals D, Hannun YA. Roles and regulation of secretory and lysosomal acid sphingomyelinase. *Cell Signal*. 2009;21(6):836–846. doi: [10.1016/j.cellsig.2009.01.026](https://doi.org/10.1016/j.cellsig.2009.01.026).
- [29] Krishnan L, Dennis Sprott G, Institute for Biological Sciences, National Research Council of Canada. Archaeosomes as self-adjuncting delivery systems for cancer vaccines. *J Drug Target*. 2003;11(8-10):515–524. doi: [10.1080/10611860410001670044](https://doi.org/10.1080/10611860410001670044).
- [30] Jia Y, Akache B, Deschatelets L, et al. A comparison of the immune responses induced by antigens in three different Archaeosome-Based vaccine formulations. *Int J Pharm*. 2019;561:187–196. doi: [10.1016/j.ijpharm.2019.02.041](https://doi.org/10.1016/j.ijpharm.2019.02.041).
- [31] Zavec AB, Ota A, Zupancic T, et al. Archaeosomes can efficiently deliver different types of cargo into epithelial cells grown in vitro. *J Biotechnol*. 2014;192Pt A:130–135. doi: [10.1016/j.jbiotec.2014.09.015](https://doi.org/10.1016/j.jbiotec.2014.09.015).
- [32] Krishnan L, Dicaire CJ, Patel GB, et al. Archaeosome vaccine adjuvants induce strong humoral, cell-mediated, and memory responses: Comparison to conventional liposomes and alum. *Infect Immun*. 2000;68(1):54–63. doi: [10.1128/IAI.68.1.54-63.2000](https://doi.org/10.1128/IAI.68.1.54-63.2000).
- [33] van Uiterl I, Le Gac S, van den Berg A. The influence of different membrane components on the electrical stability of bilayer lipid membranes. *Biochim Biophys Acta*. 2010;1798(1):21–31. doi: [10.1016/j.bbamem.2009.10.003](https://doi.org/10.1016/j.bbamem.2009.10.003).
- [34] Burade V, Bhowmick S, Maiti K, et al. Lipodox® (generic doxorubicin hydrochloride liposome injection): In vivo efficacy and bioequivalence versus caelyx® (doxorubicin hydrochloride liposome injection) in human mammary carcinoma (MX-1) xenograft and syngeneic fibrosarcoma (WEHI 164) mouse models. *BMC Cancer*. 2017;17(1):405. doi: [10.1186/s12885-017-3377-3](https://doi.org/10.1186/s12885-017-3377-3).

Appendices

Appendix 1: TLC analysis of 50 µg and 100 µg of lipids isolated from *Aeropyrum pernix* as described by **ota et al.** (2012)¹²



Appendix 2

Chromatogram of isolated polar lipids from *A. pernix*. The analysis was performed using LC-MS in positive ionization mode. The sample shows two main peaks corresponding that correspond to C_{25,25}-archetidyl(gluco)syl)inositol and C_{25,25}-archetidylinositol. Polar lipids isolated from Archaea were dissolved in chloroform, yielding a transparent polar fraction. The sample was dried, weighed, and resuspended in MeOH:CHCl₃ (7:3, v/v) to a final concentration of 1 mg/mL. LC-MS analysis was performed with a 2 µL injection volume. Each sample was injected three times in random order using full-scan acquisition in both positive and negative ionization modes. Data-dependent acquisition was used to obtain MS/MS spectra for compound annotation, with periodic injections of a standard lipid mixture for instrument performance monitoring and lipid identification. Details of the LC-MS method, data processing and compound annotation can be found in this manuscript: Mar Garcia-Aloy et al. 2023, Untargeted lipidomic profiling of grapes highlights the importance of modified lipid species beyond the traditional compound classes, Food Chemistry, Volume 410, 135360, ISSN 0308-8146, <https://doi.org/10.1016/j.foodchem.2022.135360>. (<https://www.sciencedirect.com/science/article/pii/S0308814622033222>)

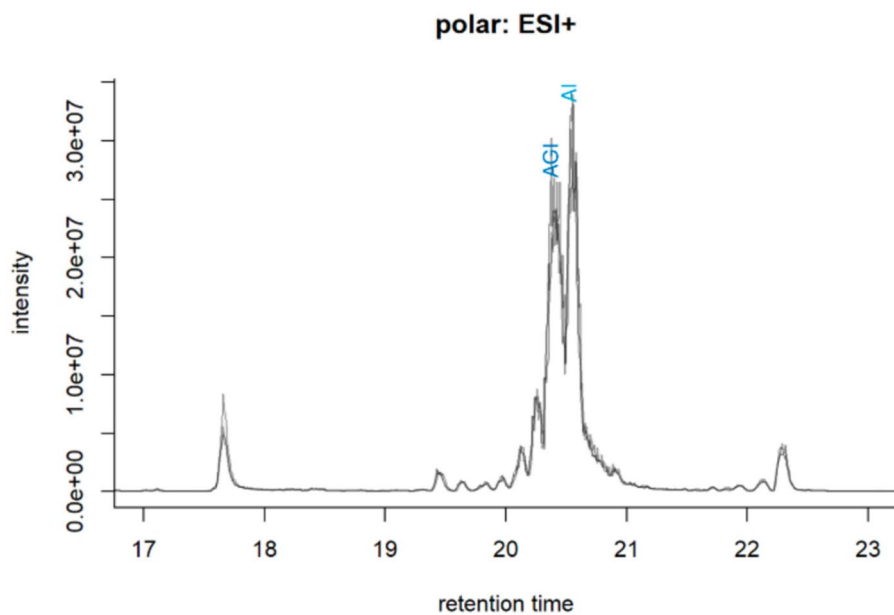
Appendix 3

Measured size and PDI of LUV samples prepared by extrusion (100 nm pore size membrane) with different lipid compositions according to Table 1.

Sample	Mean diameter ± SD (nm)	PDI
A100	143.0 ± 41.2	0.056
A0	154.5 ± 54.6	0.099
A2	163.7 ± 60.5	0.113
A5	143.3 ± 45.6	0.083
A15	151.6 ± 63.0	0.108
A25	145.0 ± 45.4	0.084
A35	145.0 ± 42.9	0.061
A45	140.0 ± 46.2	0.080

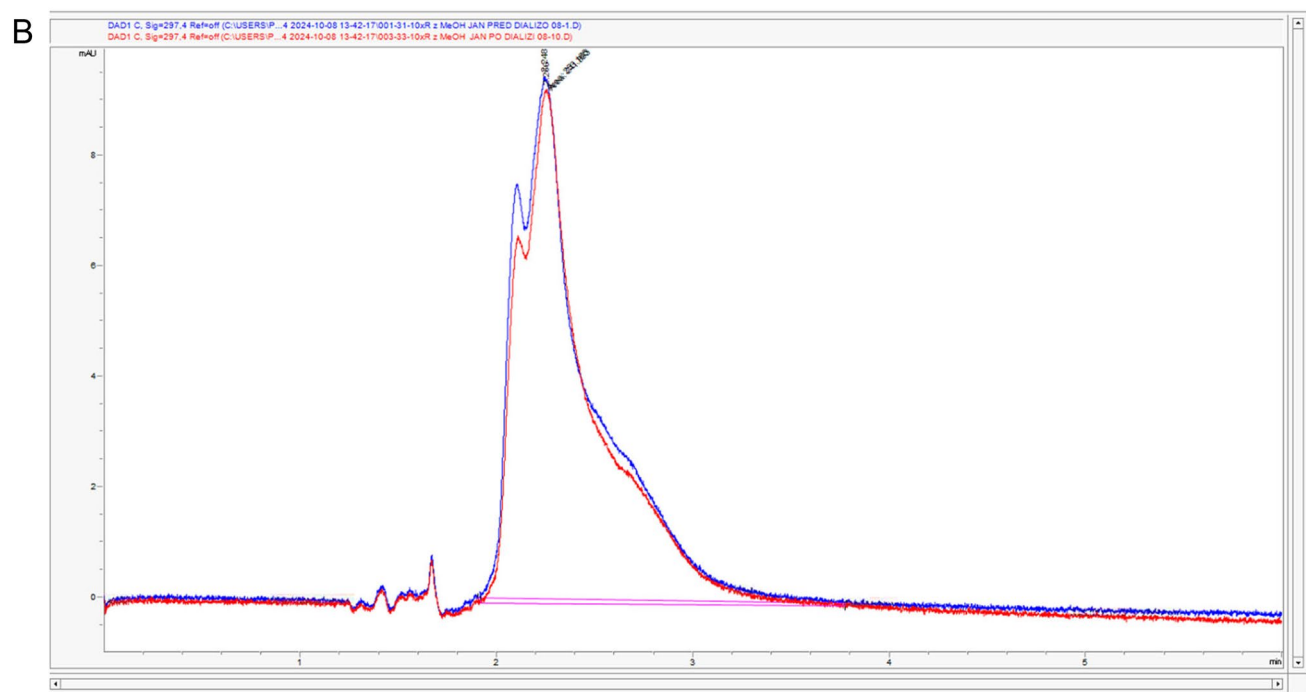
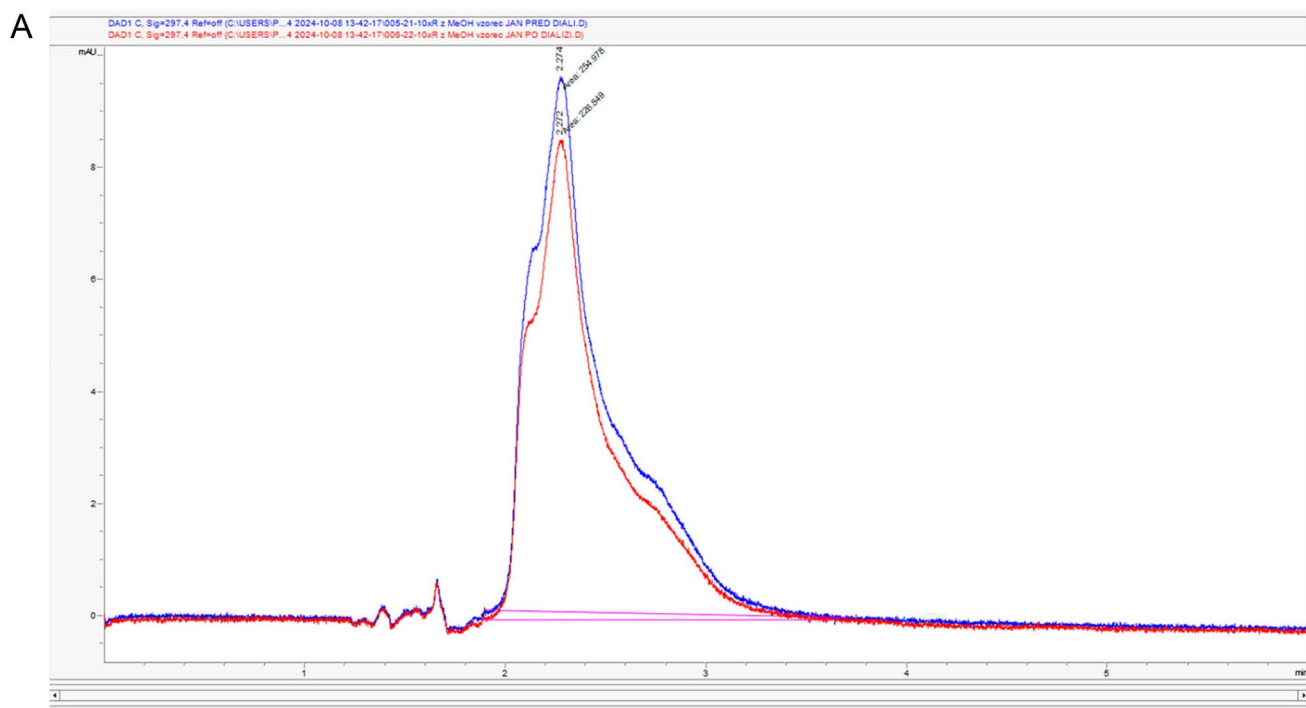
Appendix 4A

Chromatogram of released VCR after active loading before dialysis (blue) and after dialysis (red) for the LUV sample composed of an SM:CH mixture at a molar ratio of 1.5:1 (A0).



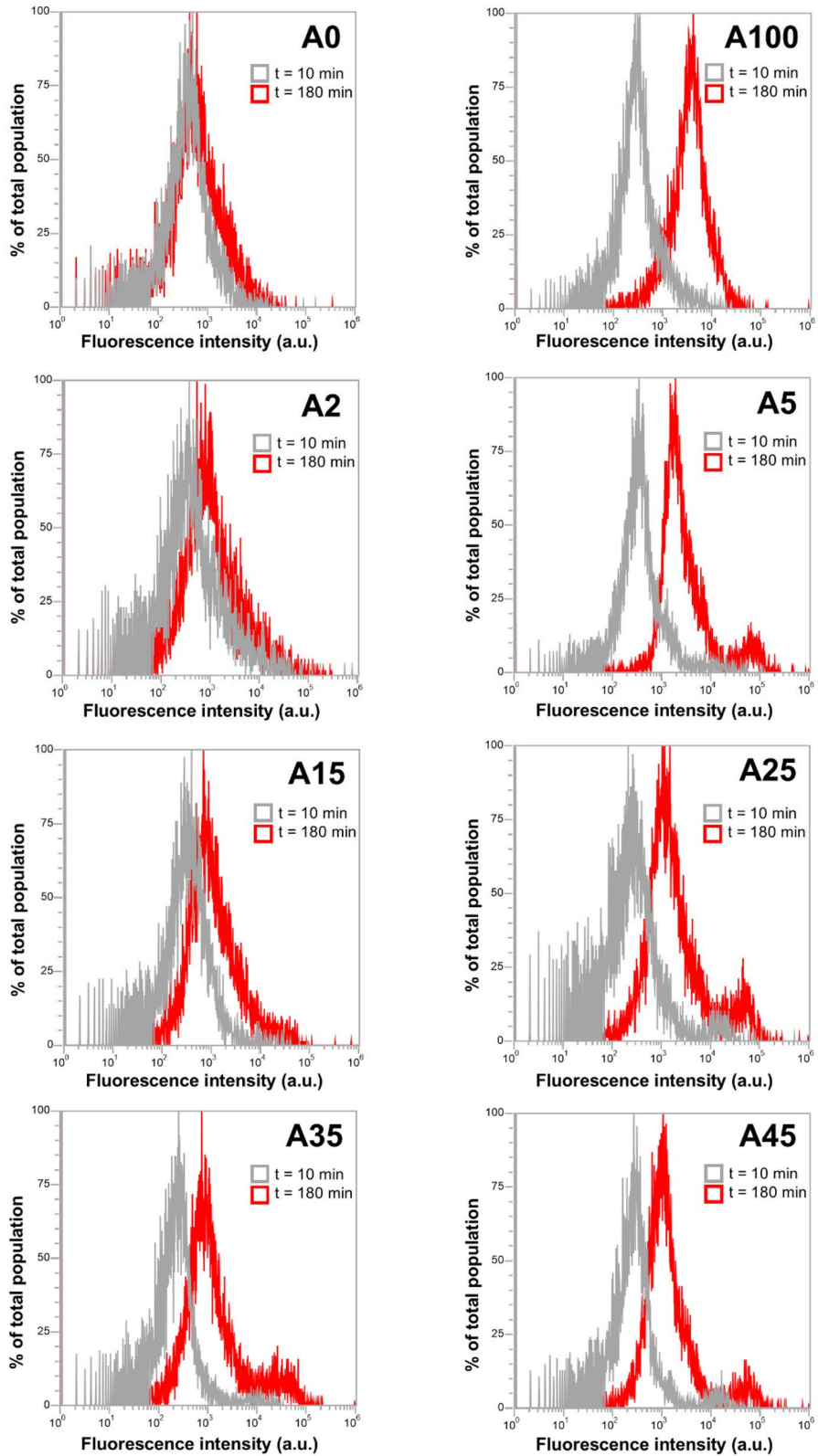
Appendix 4B

Chromatogram of released VCR after active loading before dialysis (blue) and after dialysis (red) for the LUV sample composed of a $C_{25,25}$:SM:CH mixture with 2 mol% $C_{25,25}$ and SM:CH at a constant molar ratio of 1.5:1 (A2).



Appendix 5

Fluorescence signal of CHO cells, measured by flow cytometry, reflects the release of encapsulated calcein from LUV samples after 10 and 180 min of incubation with CHO cells at 37°C.



Appendix 6

Micrograph of CHO cells showing the fluorescence signal of calcein after the addition of 1% Triton X, from the LUV sample following 24-h incubation with CHO cells at 37°C. The sample composition consisted of a mixture of SM and CH in a molar ratio of 1.5:1 with an additional 2 mol% of archaeal lipids (C2).

